OPCMG ESR

Optimal CMG Guidance

AOCS

Doc. Reference:	OPCMG-OSE-RP-2149	Project Abbreviation:	OPCMG
Issue:	01	Issue Date:	2024-11-04
State:	Released		
DRL Reference:	ESR	CI-number:	N/A

Action	Name	Function
Author:	OHB Sweden / DLR	Per Bodin
Authorised by:	Per Bodin	PM

OHB Sweden AB
P.O. Box 1269
SE-164 29 KISTA
Sweden
Tel: +46 8 121 40 100
www.ohb-sweden.se

OHB Sweden certifies that this document has been approved and signed by the above persons via an electronic approval process supported by OHB Sweden's PLM System. Document Release is indicated by the Issue Date and State "Released" written on the front page by the PLM system.

OPTIMAL CMG GUIDANCE

P. Bodin [(1)], D. Seelbinder [(2)], J. Garrido [(2)], N. Deslaef [(3)]

[(1)]OHB Sweden, Kista, Sweden, per.bodin@ohb-sweden.se

[(2)]DLR, Bremen, Germany, david.seelbinder@dlr.de

[(3)]ESTEC/ESA, Noordwijk, The Netherlands, nicolas.deslaef@esa.int

ABSTRACT

The work presented in this paper summarizes the results from a recently completed ESA study on Autonomous and Optimized Agile Attitude Control with CMGs for Small Satellites Platforms.

The paper presents the main findings of the study and focuses on attitude and CMG guidances based on optimization techniques. An inventory and selection of optimization technique is presented in the paper taking into account also CMG specific considerations and based on these findings, a guidance strategy is selected.

Mission requirements were defined for an agile modification of the on-going EIS IOD/IOV ESA development and suitable CMG units were selected and accommodated for this application based on a trade-off analysis.

A comparison was then made between separate optimization of the attitude and CMG guidances on one hand and the optimization of the complete attitude and CMG system on the other.

The overall approach was evaluated on a detailed simulator as well as on a flight-like hardware processor. The results from these simulations are presented in the paper together with some conclusions.

1 INTRODUCTION

There is currently a strong trend for satellite miniaturization with Earth Observation imaging payloads with increasing expectations in tracking and agility capabilities also for such small missions. Applications include maritime security and disaster monitoring. These are applications for which agile capabilities enable drastic enhancements in the image coverage and revisit performances.

One key element for providing agility is the actuators' torque capability and Control Moment Gyroscopes are an ideal candidate, since they provide potentially better mass and power efficiency than Reaction Wheels.

2 SELECTION OF GUIDANCE TECHNIQUE

2.1 Convex Programming

The use of numerical optimization has experienced a huge acceleration over the last years. Convex Optimization is appealing mainly for four reasons: first, for convex problems the local optimum (e.g., a minimum or a maximum) is also the global optimum. Second, very efficient general-purpose and highly dedicated solvers exist, as we will see later in this section. Third, the dependency on initial

guesses is from a mathematical point of view completely lifted, even though still useful from a numerical perspective.

Convex optimization methods are flexible enough to permit the modelling of a huge number of problems of practical interest [1], [2]. A particularly successful category of problems, the Second-Order Cone Programming (SOCP) problem is a generalization of quadratic programming that includes the possibility of embedding conic constraints in the formulation. This type of formulation has been widely used in many fields, and with particular success in GNC, especially for guidance applications (e.g., powered-descent and landing guidance [3], [4], [5], and atmospheric re-entry). More notably, this technology has been successfully employed on several rockets and vehicles, including the Falcon 9 [6] and the experimental DLR vehicle EAGLE [7], [8].

The next more general level of convex optimization is represented by Semidefinite Programming (SDP), which deals with the minimization or maximization of linear combination of positive semidefinite matrices subject to Linear Matrix Inequalities (LMIs).

These techniques found large applications in guidance, control and estimation. For example, in the work of Wang and Grant [9] the atmospheric entry guidance problem was formulated as sequence of SDPs, whereas Manchester and Peck applied SDP-based methods to the problem of estimating the inertia matrix of a spacecraft [10]. Moreover, LMIs have been largely used in control theory. The theoretical foundation for the use of LMIs in control can be found in the work of Boyd [11], and since then their use in modern control has seen a large increase. For example, the application of LMIs to the problem of synthesizing $\mathcal{H}_\infty$ controllers have been addressed by Gahinet and Apkarian [12].

Concerning CMG control allocation, it is noteworthy that matrix valued constraints, such as lower bounds on matrix norms and lower bounds on determinants can be formulated as SDP [13], [14]. Thus, if the CMG control allocation problem would be treated as SDP, the internal singularity arising from rank deficiency of the control effectiveness matrix could be explicitly prevented by including an appropriate, matrix valued constraint in the optimization problem.

The upper level with respect to SDP is finally represented by Conic Programming (CP), which focuses on linear inequalities acting on variables belonging to convex cones and operates with matrices that are not necessarily semidefinite positive [14].

2.2 Nonconvex Programming

The best and preferred handling of nonconvex constraints is through (lossless) convexification (e.g. [3]). However, such treatment is not universally possible. Sometimes an approximate, lossy convexification is possible, but if that negatively impacts performance it opposes using an optimization routine in the first place. If neither is acceptable, the non-convex constraint must be treated through linearization.

In all methods of gradient based optimization, it is required at some point to linearize nonlinear constraints to be able to evaluate the conditions of optimality. We compare how different methods prepare, augment or transform the nonlinear constraints before the linearization is performed: The most categorical difference is whether nonlinear constraints are addressed during the transcription of an optimal control problem, before it is transformed into a static optimization problem, or if the nonlinear constraints enter the static optimization problem directly. The former case leads to the recently surfacing methods of successive convexification [15], [16], [17], [18], [19] and successive convex programming [20], [21], (we use the terms successive convexification and successive convex programming interchangeably, abbreviated as SCvx). The latter leads to a nonlinear programming problem (NLP).

NLP methods solve static optimization problems with nonlinear constraints. It doesn't matter if those constraints originate from an optimal control problem or not. The physical interpretation of the constraint equations is not used during the solution process. While this makes NLP strategies generic and widely applicable, the linearization can lead to non-convex sub-problems which require regularization or other recovery strategies. This makes it difficult to prove convergence properties, hence it is not focused on in this survey.

Part of the success of convex optimization is certainly due to the availability of modern numerical methods to deal with it. Beyond the already mentioned CVXOPT and qpOASES, it is worth mentioning ECOS [22]. ECOS implements a standard primal-dual Mehortra predictor-corrector solver, but with search directions found by solving a symmetric indefinite KKT system. The system of equations is solved by applying state-of-the-art LDL factorization and elimination of the numerical determination of pivoting sequence for improving the performance of the solver. An even more customized solver for SOCPs to be employed in embedded solutions has been proposed by Dueri et al. [23]. Given the known structure of the problem the interior-point method could be carefully tailored for the specific problem to be solved, leading to drastically lower times if compared to general-purpose embedded solvers.

2.3 CMG Specific Considerations

The following section will try to show the most relevant approach on how to handle the CMG based attitude control problem within an optimization framework. First, it is listing some recent research publications which might have a direct influence on the optimization problem formulation for the later tasks. Afterwards it points to the general approach on how to solve the CMG attitude control problem.

Elliot - Momentum Control Systems and Their Application in Robotic Systems

In his PhD thesis [24] and several supporting papers [25], [26], [27] Elliot et. al. described steering laws for CMGs.

They typically concentrate on a four-CMG array in a box-90 configuration, which is equivalent to a 90° roof top configuration. They treat the description of CMG constraints in a very systematic way and develop a steering law that can avoid internal singularities and maximizes the available torque over time. This allows an attitude controller to have enough torque capability to react to disturbances. For the box-90 configuration the steering law is provided as closed-form constraint-based solution, which is guaranteed to avoid all internal singularities. What makes this reference interesting is that it bridges the gap between the robotics and CMG communities. Additionally, a list of all available singularities for three orthogonal CMG pairs is found in here. Especially the constraint formulation might become interesting for a convex optimization approach. All of these developments are linked to Honeywell's patented solution [28].

Geshnizjani – Zonotope Based Steering Laws for Agile Spacecraft with Control Moment Gyros

Geshnizjani develops in his PhD thesis [29] and accompanying papers [30], [31] a steering law for CMGs based on zonotopes. Simply speaking, zonotopes are point symmetric convex polytopes, which are used here to describe the available torque envelope of a CMG array. For this approach an arg min max optimization problem is solved which finds the optimal initial gimbal angles of a CMG array for a predefined maneuver. In principle it maximizes the available torque around the dominant axis of motion. There is even an analytical solution available when there is no angular momentum available at the beginning of the maneuver. The key element of their development is a "torque-norm" which is a measure of how much torque is available at a certain time. If their torque norm is less than

a certain value, the requested torque can be realized, otherwise it is not possible. This norm might become interesting as optimization constraint. Although many of the results that are pointed out here rely on the specific 4 CMG roof top configuration, the torque norm could be interesting for a generic optimization problem. Another important property of the roof top configuration is the connectedness of its null space, which is proven here.

The developed CMG steering law is formulated in the angular momentum/gimbal angle domain. Therefor it requires an angular momentum input which has to be provided by the attitude control loop. Instead of solving this issue by integrating a classical torque based attitude controller over one time step Geshnizjani formulates an attitude controller in the angular momentum domain. This approach simplifies the attitude control plant to the rotational error kinematics and leads to a proportional feedback control law. The choice of the proportional gain is the crucial part which has to respect the CMG array's angular momentum envelope and is solved by Geshnizjani in his PhD thesis [29].

Ramirez - Sequential Convex Programming for Optimal Line of Sight Steering in Agile Missions

This reference [32], is to the best of our knowledge, the only one which is trying to apply a convex optimization scheme to the CMG control allocation problem directly. In here the CMG control allocation and attitude control problems are addressed via a sequential convex programming approach. As a study case, a roof type setup with four CMGs is used. At the heart of the solution process a Quadratically Constraint Quadratic Problem (QCQP) solver is used, which is called by a Sequential Convex Programming (SCP) tool. Therefore, the nonlinear attitude and CMG dynamics are discretized and solved in an iterative manner until a convergence is reached. It should be noted that no convergence proof is available for this specific SCP while a convergence proof is available for problems which follow the SCVX approach according to [18]. What is interesting to mention is that Ramirez et. al. perform a variable change with the CMG gimbal angles which allows a linear parametrization of the spacecraft momentum. This exchange is shown for the specific roof top configuration, but it might be possible to have a similar exchange for the six CMG configuration as well.

Unfortunately, the developed tools are internal software development of SENER Aerospace and not freely available on the market. Nevertheless, this reference is pointing into a promising direction to utilize convex optimization for CMG control allocation.

2.3.1 CMG Control Allocation

We must differentiate between CMG steering laws that can be expressed in closed, analytic form, and steering laws that require to numerically solve an optimization problem in every time step. Closed form steering laws follow a pseudoinverse steering logic in which the gimbal rates as computed as the pseudoinverse of the Jacobian matrix of the total angular momentum with respect to the gimbal angles (e.g. [33]). The pseudoinverse can be computed analytically, thus resulting in a closed form expression for a feedback law. The singularity avoidance in the pseudoinverse steering logic is based on intelligent regularization/alteration of the Moore-Penrose pseudo inverse, which can be interpreted as artificially misaligning the commanded torque vector from the singular directions, for example the Singular Robust Inverse [34] consists in modifying the Moore-Penrose solution by adding a term which can depend on the determinant in order to maintain an invertible matrix. The Singular Direction Avoidance method [35] augments the law by steering with respect to the singular values of the Jacobian matrix. There are multiple variants and further augmentation to these methods that are not reviewed in detail. Steering laws that manage the null space motion "on the fly" make it difficult to predict a-priori how much torque will be available at a given time. To counter this a mapping can be

created in advance that defines for each position in 3-dimensional momentum space (range space) where we should be in null space. The array is then controlled to follow this mapping. This allows to predict system performance but can become complex for null space dimensions >> 1. The Moore-Penrose pseudo inverse steering law is obtained as the (closed-form) solution of a least square optimization problem

Some of the augmented steering laws are obtained as the solution of augmented optimization problems, i.e. the "Singular Avoidance Steering Logic" [36] is obtained as the solution of a weighted norm and least squares minimization.

These approaches have in common that they do not consider constraints on the gimbal rates, which enables the closed form solution. If one is willing to sacrifice the closed-form feedback law, and numerically solve an optimization problem in every control cycle, the underlying optimization problem can be expanded to include e.g. constraints on the gimbal rates and constraints to explicitly avoid singular CMG configurations. For a general overview [37] gives a survey of control allocation methods, including e.g. linear and quadratic programming approaches. For CMGs specifically however, we could not find literature references that report using computational, numerical optimization-based control allocation/steering laws. If this route should be explored the first question is: In which complexity class should the control allocation problem be formulated? The determining factor is how to incorporate singularity avoidance. For this there are three conceptual ideas:

1. Singularity avoidance through second-order cones
2. Singularity avoidance by tracking Jacobian condition
3. The third approach follows the so called max-det optimization, e.g. [13].

2.3.2 Attitude Maneuver Optimization

Within the ESA study Attitude Guidance using Onboard Optimization (AGOO) [38] the consortium developed solutions and techniques for the missions of THESEUS (Amati, et al., 2018) and Comet Interceptor [39] as reference cases. A modification and adaptation of the AGOO study results is the baseline for this study.

While CMG control allocation can be naturally treated as a static optimization problem, attitude maneuver planning is a dynamic optimization problem, i.e. an optimal control problem, that requires transcription to obtain a static optimization problem. DLR maintains multiple transcription codes based on multiple-shooting and pseudo-spectral methods that can transform optimal control problems to standardized interfaces for different complexity classes.

Depending on treatment of dynamics and constraints attitude guidance problems can be formulated in different complexity classes. For the intended use case of agile maneuvers in this study however, maneuver time optimization is an important goal. Finding a minimal time solution constitutes an optimal control problem with "free final time" which through the necessary associated transformations always results in at least bi-linear dependencies between optimization variables, thus a technique that can cope with this demand is necessary.

Initial- and/or final time dependency can be addressed in non-convex optimization by including them as optimization variables, or it can be addressed by keeping the process duration fixed from the perspective of the optimization problem but perform a bi-section search in an extra loop (which requires solving the fixed-time problem multiple times).

Thus, the problems of interest in this study are classified as having nonlinear (dynamic) constraints that cannot be convexified in a direct lossless manner hence, to be able to develop a strategy that can

be generalized to multiple guidance scenarios with reasonable effort, the choice of approaches is limited to nonlinear programming or successive convexification.

2.3.3 Combined Attitude Maneuver and CMG Control Allocation Optimization

There exist no dedicated optimization techniques that exploit the structure or particularities of attitude guidance and CMG steering problems specifically. That means this problem can also be treated as a deputy of its generic complexity class and the choice of optimization algorithm can be based purely on complexity class and convergence properties of the optimization algorithms for that class.

As already solving the free final time attitude guidance problem demands nonlinear programming or successive convexification, adding the control allocation does not alter the fundamental complexity class.

What is altered is the model, and specifically which states to include in the optimization. Here it seems a natural choice to include the components of the momentum vectors of every CMG as states (in addition to an attitude representation of the vehicle). To guarantee a smooth control it is an option to also treat the gimbal rates as additional states and use the gimbal acceleration as the control variables, which will also allow to limit the maximal gimbal acceleration.

By going from the pointwise, static control allocation (i.e. feedback) to a single prediction-based planning including the control allocation, the impact of having a good singularity avoidance is reduced. A feasible solution of the Optimal Control Problem (OCP) implies that the maneuver planning (including CMG steering at every discretization point) is feasible and that the boundary conditions are satisfied. This may involve that during the maneuver the CMG array enters a singular configuration.

In fact, it is likely that time optimal solutions contain at least a contact point with the singular hull, because the control system is going to operate at the limit to achieve time optimality. However, a conservative engineer might not be willing to accept that. Then it comes back to the discussion on constraint-based singularity avoidance. Naturally conic exclusion constraints can be included at every discretization node, effectively imposing the internal singularity avoidance as a path constraint in the OCP formulation. The same is theoretically possible for a lower determinant bound on M, this would lead to a LMI formulation.

2.3.4 Kernel/Nullspace

One important aspect in CMG control algorithms is to understand and utilize the null space. The null space is, simply speaking, the degree of freedom the CMGs gimbals can rotate without transferring a torque onto the satellite. Therefore, it can be used to avoid singularities and to reconfigure a CMG array. As long as there is a null space existing for the selected CMG array, there are possibilities to navigate the CMGs gimbals through it, but there are several restrictions to it. It could occur that the null space of a specific structural CMG arrangement is not connected and therefore it does not allow a smooth transition form on point of the null space to another one. This means in general a CMG array cannot be reconfigured without transferring torque onto the satellite.

2.4 Strategy Selection

For on-board CMG control allocation, we think that a closed-form feedback law with singularity avoidance, such as e.g. [36] or [28] is the best choice. Depending on the required control allocation frequency, even convex problems might be too computationally expensive to meet hard real-time deadlines.

The disadvantage of the closed form steering laws is that they cannot obey limits on gimbal acceleration and thus gimbal rate change can be very steep. However, this is mitigated by the fact, that the steering law should be used together with a feedforward solution (from the attitude maneuver optimization) that considers and obeys the torque limits of the CMG array.

Our conclusion for solving on-board minimal time attitude guidance problems is to use a successive convexification approach, inspired by the work of [17] and [20].

The conclusion for the combined attitude guidance and CMG allocation problem is the same as for the stand-alone online attitude optimization, because the complexity of the control allocation is dominated by the complexity required for the attitude guidance. Thus, adding the control allocation will complicate the problem formulation, but not change complexity class of the outer SCVX problem.

3 MISSION AND REQUIREMENTS DEFINITION

3.1 Mission Definition

This section defines the mission that will be used in this study to demonstrate the use of the CMG algorithm. The mission is based on the on-going OHB Sweden project EIS which is an ESA project for the flight demonstration of a multispectral imager. The spacecraft platform is based on the OSE InnoSat platform. This section provides an overview of the EIS mission, system architecture, and AOCS. The key elements to consider for the adaptation of the spacecraft into an agile platform using CMGs in place of normal RWs. Finally, the section presents the baseline agile mission resulting from the adaptation.

OHB Sweden is currently developing the EIS IOD/IOV mission under ESA contract [40]. The contract covers the procurement of one spacecraft accommodating the ELOIS hyperspectral imager experiment. The experiment is pre-selected by the European Commission as part of an objective to promote European competitiveness and non-dependence. The mission is implemented through the EIS20 spacecraft which is based on OHB Sweden's existing microsatellite platform InnoSat with adaptations for the EIS mission. See Figure 1 for a picture of the preliminary EIS20 spacecraft hosting the ELOIS instrument.

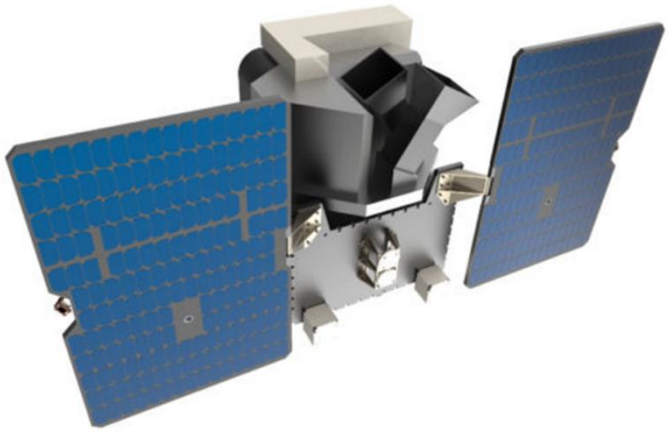

Figure 1: Left: EIS20 spacecraft. Right: ELOIS instrument.

ELOIS is an Earth observation VNIR/SWNIR spectrometer [41] developed for a Hyperspectral remote sensing mission by AMOS.

The EIS platform and AOCS are briefly described in [42]

The following key elements need to be considered for an adaptation of the EIS20 spacecraft to an agile version of the EIS mission:

Momentum Control System

The current EIS20 baseline AOCS includes a set of four hot redundant Reaction Wheels with a unit capacity of 0.4 Nms. The unit mass is 0.8 kg and the power consumption is 2 W in standby, 5W in steady-state at high speed and 20 W maximum power consumption. As part of the key subject of this study, the RW assembly will be replaced with a set of suitable CMG units for which the delta mass and power will be assessed.

Attitude Determination

The Gyro used on EIS20 is an adaptation compared with the standard InnoSat equipment and is selected for the EIS20 spacecraft to meet the challenging pointing requirements. It is expected that the units will be sufficient also for an agile version of EIS.

Data Handling System

For an agile mission, the required capacity of the DHS is driven by the need to perform on-board optimization to compute the attitude guidance as well as the CMG control. In addition, an agile mission may require a higher AOCS sampling rate to be able to efficiently control flexible mode resonances. The results from this study will determine if there is a need to replace the current on-board computer with one that is based on e.g. an LEON4 processor.

Power System

It is expected that the introduction of CMGs will result in an increased power capacity need.

Structure

Adaptations to the structure are expected to be able to accommodate the mass and volume of the CMG units as these are expected to require a larger volume than what is needed for the RW units currently baselined. However, initial assessment indicates that structural adaptations are expected to be limited to internal modifications and that the external envelope of EIS20 will remain the same.

3.2 Mission Requirements

An agile spacecraft can perform different types of pointing such as multiple target collection, multiple strip imaging, stereo or tri-stereo imaging, and corridor acquisition. The agile scenarios to be considered in this study are required to include a multi-strip scenario.

To obtain an initial iteration of what would be required for such a scenario, it was investigated how many parallel strips could be handled in practice.

The same ground track velocity as in the nadir pointing case is assumed and the strips are aligned North/South. Each strip is assumed to have a time interval in the beginning and a time interval in the end that are allocated to slewing. The sum of these times is denoted as the slew time. Following the initial slew interval, there is a tranquillization time interval. The rest of the strip is allocated for imaging. See Figure 2 for an illustration.

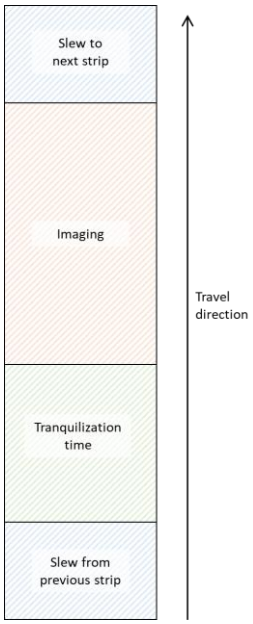

Figure 2: Parts of imaging strip.

The maximum off-nadir angle in EIS20 is 30°. The same angle is assumed for EIS-agile but here as a half-cone angle from nadir.

MIS-AGL-0010 During imaging, the spacecraft ELOIS instrument LoS shall not deviate more than 30° from nadir.

Taking this constraint into account, it was investigated how many parallel strips could be accommodated and it was concluded that not more than 3 parallel strips is practical.

MIS-AGL-0020 The spacecraft shall be able to perform multi-strip imaging with a minimum of 3 parallel strips.

Assuming three parallel strips, it was further investigated what is the obtainable length of the imaging part of the strip assuming slew, and tranquilization times.

The factor of four is included to allow for a more active control of solar panel flexible modes.

Based on the performance of the ELOIS instrument we assume the following APE and RPE.

MIS-PNT-0020 During imaging, the APE shall be less than 5” per axis with 99.73% confidence with temporal statistical interpretation.

Note: This requirement excludes all bias errors.

MIS-PNT-0030 During imaging, the RPE shall be less than 3” over 5 s and less than 0.15” over 7 ms, per axis with 99.73% confidence with temporal statistical interpretation.

3.3 CMG Selection

This section provides the background for the CMG selection. The section includes a brief review of the small CMG market followed by the identification of the most important selection criteria. A trade-off summary is then provided followed by a proposed selection of dual CMG source.

A comparison of CMGs and RWs was provided in [43]. A corresponding comparison performed for this document is summarized in Figure 3.

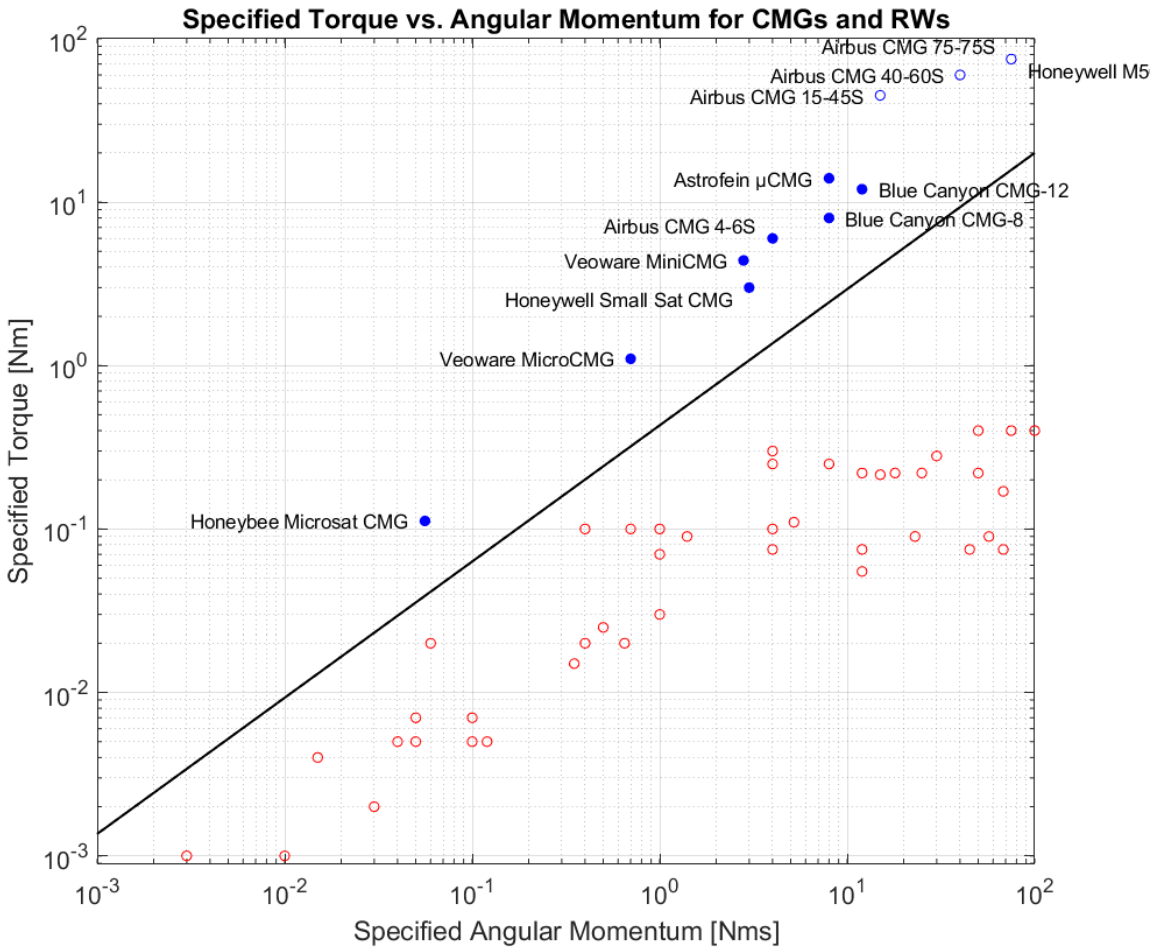

Figure 3: Reaction wheel and CMG torque and momentum comparison.

The figure shows the angular momentum vs. torque for the CMG providers that seem available and for completion, the corresponding data is shown for ordinary reaction wheels. The figure shows CMG data in blue and RW data in red. The RW data is supplied to demonstrate the difference and separation in performance between the two types of actuators.

The CMG providers found are Airbus, Honeywell, Astrofein, Blue Canyon, Veoware, and Honeybee. In addition to the units shown in Figure 3, there is also a number of CMGs developed for different cubesat projects as reported in e.g. [44]. These are however not considered for this study because of their small size and low TRL or limited availability. There is also a number of lower-TRL units under development in the range suitable for small satellites, where the 5 Nms/ 5 Nm JMG-050 from Justek, the 3 Nms MiniCMG from TAS-I developed for PLATiNO, and a 3 Nms unit under development from Honeywell (Czech Republic) are worth mentioning. Information for these units is however very limited.

There is also a number of units developed by the Research Institute of Command Instruments (Научно-исследовательский институт командных приборов), St. Petersburg, Russia; see [45]. These units range from 3 to 250 Nms and 1 to 100 Nm. The development status and availability of the smaller unit may be interesting to investigate further.

The providers of the RW units indicated in the figure are Honeywell, Collins Aerospace, Astrofein, Blue Canyon, Sinclair Interplanetary, NewSpace Systems, and Veoware. The figure also shows a black line to demonstrate the separation between CMG and RW. The solid blue dots in the figure indicate CMGs suitable for small satellites.

The key performances of the CMG units considered are summarized in Table 1.

The table also provides the momentum to mass ratio and the torque to mass ratio since these metrics are often used to analyze the efficiency of CMG units. The analysis of the CMG unit does not include the available gimbal acceleration since it is not available in the datasheets. This information does not directly influence the choice of the CMG unit. The gimbal acceleration for the selected units will be made available and used in the modelling and simulation of the CMG units.

For a CMG, the gimbal angular acceleration corresponds to the derivative of the torque, also called the "jerk"; see [46].

Manufacturer	Model	Momentum [Nms]	Torque [Nm]	Nominal/ Peak Power [W]	Mass [kg]	Dimensions [mm]	Volume [dm³]	Momentum/ Mass Ratio	Torque/ Mass Ratio
Airbus	4-6S	4	6	6 / 64	13	270×225×313*	19	0.308	0.462
Astrofein	µCMG	8	14	20 / 40	8	188×188×240†	8.5†	1.000	1.750
Veoware	MiniCMG	2.8	4.4	11 / 45	3.25	120×120×185†	2.7†	0.862	1.354
Veoware	MicroCMG	0.7	1.1	11 / 30	2.75	97×97×180†	1.7†	0.255	0.400
Blue Canyon	CMG-12	12	12	20 / 35	15	340×43×380*	5.6	0.800	0.800
Blue Canyon	CMG-8	8	8	15 / 30	N/A	N/A	N/A	N/A	N/A
Honeybee	Microsat CMG	0.056	0.112	1.5 / 2.0	0.775	48×49×91 215×115×25‡	0.22	0.072	0.145
Honeywell	Small Sat CMG	3	3	10 / 15	3.4	120×120×210§	3.0§	0.99	0.99

Table 1: Summary of CMG key performances.

For the selection of the CMG, the following parameters of the mission are considered,

- Momentum/Torque for the EIS-agile mission, and that is also suitable for the small satellite platform onwards
- Mass / Volume
    - The current EIS-agile design can accommodate a box corresponding to the 438×312×186 mm of the Veoware MiniCMG cluster using the perpendicular case. This corresponds to 25.4 dm^3 and shall be used as the dimension / volume requirement. The exact volume and dimensions should be investigated per case as the packaging may allow further volume if placed differently.

* Missing information on electronics dimensions / volume.
† The electronics are integrated in the CMG.
‡ Separate electronics for a 4 CMG cluster.
§ Separate electronics, missing information on dimensions / volume required.

- Power consumption: The EIS RW unit mass is 0.8 kg and the power consumption is 2 W in standby, 5 W in steady-state at high speed and 20 W maximum power consumption. The corresponding assembly of four reaction wheels for comparison will thus be 2.8 kg, 20 W nominal / 80 W peak.

The summary of trade-off results shows that the two Veoware CMGs and the Honeywell Small Sat CMG will fit the specification. The Honeybee momentum/torque capability is considered to be too low. The Airbus, Astrofein and Blue Canyon CMG-12 are overly sized and will add unnecessary mass / volume to the platform. Information from Blue Canyon has not been possible to receive for CMG-8 and CMG-12.

As described above, the Veoware MiniCMG will be preferred over the MicroCMG since the MiniCMG and the Honeywell Small Sat CMG both provide a very similar specification that make them interchangeable in analysis and in the accommodation.

The estimated power usage of all possible CMG all exceeds the power usage 20 / 80 W of a reaction wheel assembly. The intention is to extend the solar array assembly to provide relevant mass properties for the spacecraft.

3.4 CMG Accommodation

The CMG cluster can be associated with a pyramid having equidistant triangular base and there the gimbal axes of each CMG pair are normal to the pyramid sides. The pyramid angle is the (minimum) angle between the pyramid height vector and any of the pyramid sides. The alignment of the CMGs is illustrated with Figure 4. The pyramid can be parameterized by the angle θ as defined in the figure.

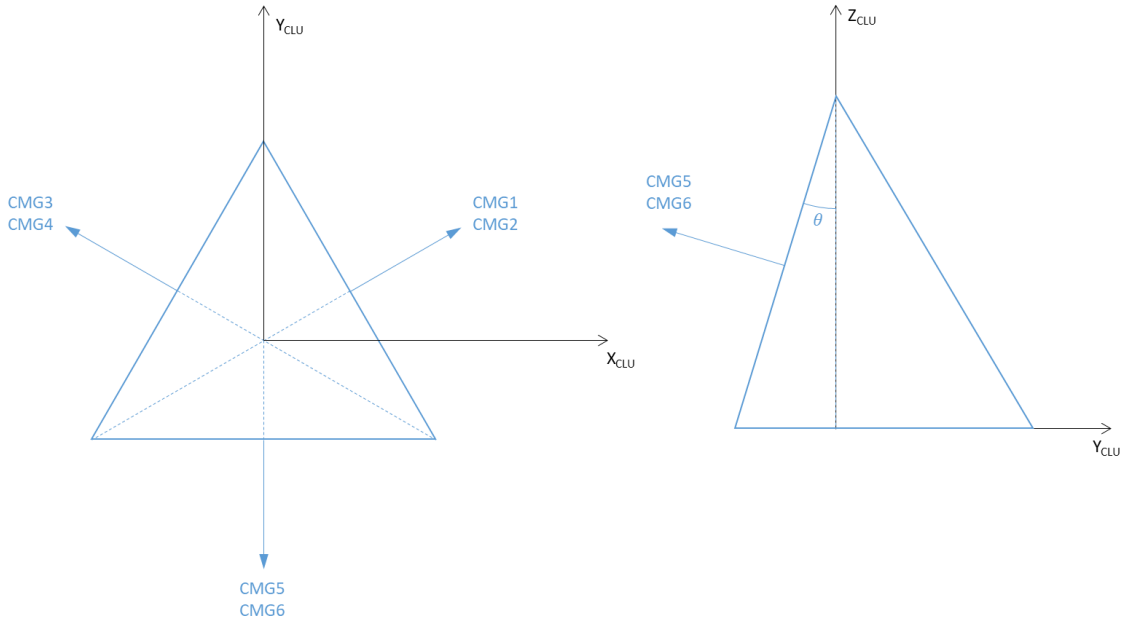

Figure 4: Illustration of CMG pyramid alignment.

It is possible to show that with

$$\theta = \frac{1}{2}\arccos\frac{1}{3} \approx 35.26\,^\circ \tag{3.1}$$

the three pairs of gimbal vectors become orthogonal.

The orthogonal pyramid case is favored for several reasons. The envelope volume of this configuration is minimum with the best "packing" of the CMG units. In addition, the secondary structures needed (if any) for mounting the units becomes significantly simpler since no manufacturing of brackets with non-perpendicular angles will be needed.

There are other advantages from implementing the orthogonal accommodation. The command allocation geometry becomes simpler in general but in particular, this accommodation allows for restricted capacity operation for the 6-CMG cluster in a way similar to the restricted operation explained in [46]. Such operation allows for a pre-selected kernel and a deterministic "fixed-map" operation of the units.

4 INVESTIGATED STRATEGIES

We distinguish methods that

A. plan only the satellite attitude maneuver without knowledge of the CMG array dynamics

B. plan the CMG array dynamics for a given satellite attitude maneuver

C. constitute a full guidance scheme for a CMG controlled satellite

The study was based on the fundamental assumption that it is useful to separate attitude guidance from CMG array guidance to reduce complexity.

In the performed investigation a full guidance scheme (*C*) does either consist of one method from category (*A*) and one method from category (*B*), or it is a holistic approach that treats satellite attitude and CMG array guidance together.

4.1 SatGui0: Combined nonconvex optimization of satellite attitude and CMG array

We start by introducing the holistic approach in which satellite attitude and CMG array guidance are treated together. This method employs numerical nonconvex optimization to solve a free final time nonlinear optimal control problem to find the gimbal angle rate trajectory that turns a satellite in the shortest possible time (or variations thereof) in the desired way. This approach, if successful, defines the performance limit, and thus the benchmark against which all other methods compare. While qualitatively this is undoubtedly the best approach, it is also the most difficult to implement onboard. In addition to the known risks of nonconvex optimization on real-time systems, this approach suffers from the particularities of the OCP formulation that describes the CMG array. The pyramid CMG array has a 3-dimensional nullspace and a state dependent control space, which create a solution space that has many local minima of hugely varying objective values. Thus, the numerical optimization of this problem does often not find the global optimum, and not even a "good" local minimum. When starting without an initial guess the procedure may require human steering or parameter tuning to converge to an acceptable solution.

This on the one hand motivates the setup of the study, which tries to breakdown this complicated problem into separate parts for the attitude guidance and the CMG array guidance. And on the other hand, it motivates the development of methods, other than optimization, which might produce reasonable results that could potentially be used as initial guess, to improve the convergence. We now first outline the first approach: "Separate optimization of attitude guidance and CMG array guidance", starting with the attitude part.

4.2 AttGui1: Attitude guidance by nonconvex optimization

This method employs numerical nonconvex optimization to solve the satellite rigid body dynamics for arbitrary boundary conditions. The method is flexible in that different objectives and constraints can be incorporated. Most important is the ability to optimize the total maneuver duration through the solution of a free terminal time optimal control problem. To limit the complexity of this problem the CMG array is abstracted as an (gyroscopic) actuator that is able to provide a certain amount of torque about the axis of the satellite. The abstracted actuator enters the OCP formulation in the form of box constraints on the torque. Note that this model assumes that the available torque is a constant which is time independent and most importantly independent from the internal state of the CMG array (which should be purposefully not modelled in this formulation). However, this simplification is a fatal mistake, as will become clear shortly. Seen purely from attitude guidance perspective however, the problem is well formulated, it is possible to find a solution for arbitrary boundary conditions, and the formulation, though nonconvex, is good natured, such that the optimal solution can be reliably computed. The obtained control solution is a torque over time profile, which is given as input to the CMG array guidance.

4.3 CmgGui1: CMG array guidance by nonconvex optimization

This method is meant to be paired with AttGui1 and employs numerical nonconvex optimization to solve the CMG array dynamics to find a gimbal angle rate trajectory that produces a desired effective torque over time profile. Due to the imposed fundamental separation between attitude guidance and CMG guidance, this problem is purposefully constructed to not include a representation of the satellite attitude. The only link to the satellite attitude is the torque over time profile (input), that if applied, transfers the satellite from the initial condition to the final condition. In this setting, it is impossible for the CMG array guidance to improve upon the maneuver time given by the input torque over time profile, because if a divergence from the desired torque profile occurs, the effect on the satellite attitude is unknown within the restriction of the formulation. In fact, the best possible outcome of CmgGui1 is, that the desired torque profile can be produced exactly, which will then execute the maneuver as planned.

In addition, it is important to ask whether it is always possible to find a solution that produces a desired torque profile, and unfortunately this is not true due to the fact, that when the attitude maneuver was planned, it was assumed that the actuator can produce a fixed amount of torque at all times. In a CMG array however, the torque that can be produced in a direction depends on the state of the gimbal angles. To solve this predicament our first approach was to ask: “Is there a minimum amount of torque, that the CMG array is guaranteed to be able to produce, always?” The answer to that question is: While it is possible to maintain the CMG array through nullspace control in such a way, that torque capability is maximized, it is not possible to guarantee a positive lower bound. This can be understood when considering the situation in which the momentum vector of the CMG array is about to reach the momentum envelope. Recall, that the momentum envelope is defined as a set of states, in which the array cannot produce momentum in a given direction anymore. So, the amount of momentum that a CMG array can produce in a given direction is finite (different from a reaction wheel). And because torque is the derivative of momentum, also the torque that can be produced about an axis is finite. And because of that, there is obviously no lower torque bound that can be achieved at all times, other than zero. This realization is extremely important, because it fundamentally invalidates all approaches to abstract the control space of the CMG array in terms of pure torque constraints!

4.4 SatGui11: Attitude and CMG array optimized separately

The combination of AttGui1 and CmgGui1 is the full guidance scheme called SatGui11. With the problems found for CmgGui1, this approach is not good, as it fundamentally cannot guarantee the satisfaction of the boundary conditions for the set of attitude maneuvers it was designed for. One can now ask, is it possible to modify and save the abstraction of the CMG array by including additional constraints, e.g. in addition limiting the total integral of torque that can be produced in any direction, in the attitude guidance formulation. But this effort is futile, as it would still not adequately describe the torque that the CMG array can produce at each time instant. The only way to obtain this information is to keep track of the individual gimbal angles themselves, which is what we set out to avoid by introducing the separation between attitude guidance and CMG guidance. Hence the conclusion is: The separated optimization of the satellite attitude and the CMG array gimbal angles does not lead to a procedure that is guaranteed to be able to satisfy arbitrary boundary conditions, which is a huge disadvantage. And this drawback is not necessarily seen in numeric testing. The benchmark maneuvers for example have a too small rotation angle in comparison to the momentum envelope of the CMG to reveal this problem. However, in our opinion this disadvantage is so significant, that it disqualifies the separated approach for general maneuvers, independently from the numeric performance it might achieve for “mild cases”, in which it works as intended

4.5 AttGui2: Eigenslew

Because of the difficulties encountered for the scheme SatGui11, and a torque over time profile apparently being a disadvantageous interface between attitude guidance and CMG array guidance, this approach simplifies the attitude maneuver planning to the Eigenslew. The Eigenslew is given by rotation about a single axis, which is constant in time, such that the interface to the CMG array guidance is reduced to the axis of rotation. This has the potential to also simplify the CMG array guidance, as now the task is reduced to “rotate as fast as possible about the given axis”. With this simplification comes the limitation that it can only be applied to rest-to-rest maneuvers, and the compromise that the Eigenslew is sub-optimal, depending on the inertia of the satellite.

4.6 CmgGui2: Iterative torque profile planning

This strategy was designed to be combined with the Eigenslew (AttGui2) and born out of the intent to also replace the optimization of the CMG array trajectory with something simpler and iteratively approach the maximum torque the CMG array can produce on the desired trajectory: This approach first analytically planes a bang-coast-bang maneuver for the rotation about the given rotation axis, using a given maximum torque. Then the dynamic system that connects the torque over time profile to momentum is solved. The gimbal rates are then computed via the pseudo inverse. Then a scaling factor is computed, such that the fastest gimbal is at the maximum rate. The scaling factor is then applied to also scale the torque limit used for the initial planning, and the procedure is repeated.

This strategy circumvents numerical optimization, but it is much more restrictive: It is only applicable to rest-to-rest maneuvers with rotation about a single axis and it does not incorporate singularity avoidance. For these restricted cases the iterative procedure was empirically found to be convergent, but it lacks a formal proof.

4.7 SatGui22: Eigenslew with Iterative torque profile planning

The combination of AttGui2 and CmgGui2 yields a guidance scheme that is guaranteed to produce a solution for arbitrary single-axis slew maneuvers that start and end at zero angular momentum. The obtained solution is not optimal because the Eigenslew is not optimal and CmgGui2 is based on the stepwise evaluation of the (saturated) pseudo inverse, which is an effort minimizing strategy, but only

for a single time step. Further drawbacks are that CmgGui2 is based on an iterative algorithm and that it lacks singularity avoidance.

4.8 CmgGui3: Predictive planning of satellite rotation angle and CMG gimbal trajectories

This strategy is also meant to be paired with the Eigenslew, i.e. it is only applicable to a rotation around a single axis. Compared to CmgGui2, we loosen the imposed separation between attitude guidance and CMG array guidance in so far, that we allow CmgGui3 to keep track of the satellite attitude in the form of the achieved rotation angle around the given rotation axis (input). In other words, internally CmgGui3 has knowledge of the satellite inertia, the satellite attitude, and the rigid body dynamics. This allows to perform a numerical prediction (forward integration) of the satellite rigid body dynamics in closed-loop with the CMG array dynamics and a CMG array control law. The control law that we choose is similar to CmgGui2 in that at its core it uses the pseudo-inverse and scales the gimbal rates, such that the fastest gimbal operates at the maximum rate. But in addition, the CmgGui3 control law also monitors a singularity avoidance criterion and is able to avoid singular points. An additional advantage over CmgGui2 is that the planning strategy is not iterative, thus convergence is guaranteed analytically.

4.9 SatGui23: Eigenslew with predictive planning of satellite rotation angle and CMG gimbal

Together with the Eigenslew CmgGui3 constitutes a guidance scheme that is able to solve arbitrary single-axis slew maneuvers that start and end at zero angular momentum. The obtained solution is not optimal because the Eigenslew is not optimal and CmgGui3 is based on the stepwise evaluation of the (saturated) pseudo inverse, which is an effort minimizing strategy, but only for a single time step. However, the control law is able to avoid singular points of the CMG array, and though based on numeric prediction, the strategy does not require iteration and in particular, does not require numerical optimization. As such this strategy is a realistic candidate for real-time onboard usage.

4.10 Qualitative Comparison of Methods

The different optimization approaches were compared, and the resulting qualitative performance assessment is straight forward and clear:

1. SatGui0 is by far the most powerful approach, if it does converge to the solution. It covers arbitrary rotations around time varying axis and is able to incorporate a wide range of additional constraints. For offline analysis and benchmarking it is undoubtedly the best choice. However, for autonomous onboard operation by itself it is not reliable enough.

2. SatGui23 is the next best choice. Compared to SatGui0 it only covers a reduced set of application cases, namely rest-to-rest single-axis rotations. Note that this in particular prevents updating the guidance solution after the maneuver has started, so this is a purely open-loop planning strategy. But the scheme is guaranteed to produce a feasible solution for all rest-to-rest single rotation axis slew maneuvers.

3. SatGui11 is a poor strategy, because it tries to cover arbitrary rotations as encoded in the torque over time profile computed by AttGui1, but CmgGui1 cannot guarantee to exactly follow this torque trajectory. In terms of convergence, this method is still in the realm of nonlinear optimization, so convergence guarantees are lacking, however the empiric experience is that it solves more reliably than SatGui0.

Based on qualitative assessment it appears that SatGui23 combined with SatGui0 could achieve the combined best of all approaches, when SatGui23 is executed first, and the solution used as initial

guess to start SatGui0. In that way, the worst-case guaranteed performance is that of SatGui23, with the potential to achieve even better performance, if SatGui0 converges to a better solution, starting from the provided non-trivial initial guess given by SatGui23.

5 PIL TESTING

Guidance strategy SatGui0 has also been successfully executed on an embedded system using the Zedboard with the Zynq-7000 ARM-based CPU; see Figure 5. The optimization problem that is being solved has 2220 free variables, 558 equality constraints, 2665 inequality constraints and 1489 conic constraints.

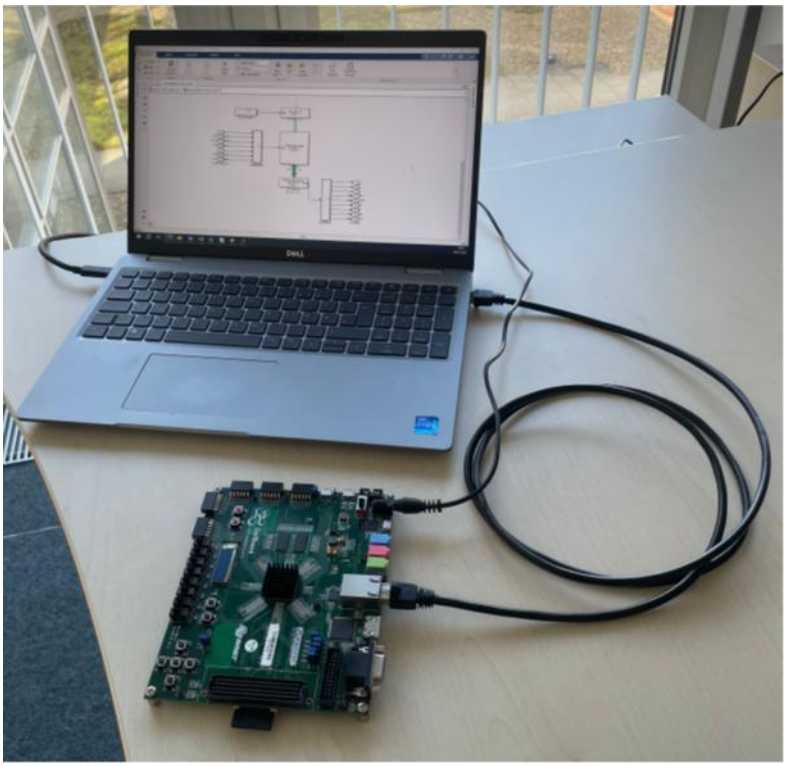

Figure 5: Setup consisting of PC connected to the Zedboard with the Zynq-7000 ARM-based CPU.

The solutions obtained on the Zedboard are qualitatively and by optical inspection identical to the solutions obtained on the host PC, however they are not numerically identical. The reason for the numerical differences is at this time unknown, likely causes are different compiler core math libraries or differing floating point number standards.

Concerning computation time, we see a significant slowdown on the Zedboard. The average computation time on the host PC is about 3.6 seconds for 50 SCvx iterations, i.e. the average time to solve a single SOCP is about 0.07 seconds.

On the Zedboard the computation time for 50 SCvx iterations is about 98 seconds, i.e. the average SCvx iteration time is about 1.96 seconds (including one execution of the SOCP solver), which is a significant slowdown by a factor of 27.

This result is in line with the data collected during the prior study “Attitude Guidance using Onboard Optimization” (AGOO) [38] in which the slowdown factor was found to be 30. The difference in pure CPU frequency is much lower: the Intel CPU uses only a 2.8 times higher tact than the Zynq-7000. CPU frequency alone is not sufficient to explain the slowdown. Other important factors are cache size, cache architecture, floating point units and instruction sets. The onboard optimization software

is demanding for an embedded system in terms of both CPU and memory use. This is likely a point in which the performance could be further improved, because with reduced memory consumption a higher portion of data fits in the CPU cache which is likely to have a positive effect. These optimizations are a continuous ongoing effort and part of future work.

The computation time to obtain the solution however significantly exceeds the maneuver duration. In particular the computation time is also much higher than the improvement of the maneuver time achieved by SatGui0 over the non-optimization based method SatGui23 for which we expect the computation time on the embedded hardware to be lower. It has to be concluded that for the practical use in a scenario of spontaneous, just-in-time maneuver computation SatGui0 is too demanding. The resulting optimization problem is quite large, it has many nonlinear constraints, and it requires 50 SCvx iterations to converge to acceptable accuracy, which results in computation times on the embedded hardware in the order of 90 seconds, which is too long for just-in-time computation. It is remarked however that the used Xilinx Zynq-7000 SoC is not the newest generation of embedded processors. The obtained results should thus be seen as a conservative bound on the expected computation time.

Qualitatively the solution obtained by SatGui0 is unmatched by other methods. If the desired maneuver is known at least 100 seconds in advance SatGui0 could still be considered to exploit the full optimality and constraint satisfaction ability. For spontaneous, just-in-time maneuver computation the non-optimization based SatGui23 approach however is preferable.

6 PERFORMANCE EVALUATION

The benchmark mission consists of a chain of rest-to-rest satellite rotations around fixed axes. The test cases defined include scattering of mass properties, CMG alignment and angular momentum. Thus, in the following performance evaluation the guidance solution has been obtained using strategy SatGui0.

The analysis provided is divided into the evaluation of control errors, pointing errors, and the commanding in terms of the properties of the gimbal angles and their rates.

Control errors

The control errors are a good indicator of the performance of the controller and demonstrate how well the controller converges. There are no actual quantitative evaluation criteria for the control error in this study.

Pointing Errors

The APE is computed as the error between the simulated attitude and the guidance attitude.

The RPE over 5 s is computed as the maximum of the APE minus the minimum of the APE over a time interval starting at the current time and ending 5 s after the current time.

The RPE over 7 ms computed as the difference between two consecutive samples of the APE. The simulation sample time is 10 ms so the error definition is adjusted to this 10 ms rather than 7 ms.

Commanding

The gimbal angles are displayed together with the guidance gimbal angles. Note that the difference is not only an error since the actual gimbal angles are a result of the gimbal rate commands resulting from the feedback attitude controller.

The gimbal rates are shown to demonstrate that the rates reach their saturation limit such that the maximum torque capability is utilized.

Slew duration

The slew durations for the guidance and resulting performance are summarized in a table.

6.1 Analysis of Performances

Control error

The control errors are summarized in two figures. Figure 6 shows an overview of the control errors for the complete simulation. Figure 7 shows the control errors during each of the four slew maneuvers. The figures show that the errors converge nicely for each of the three observation criteria.

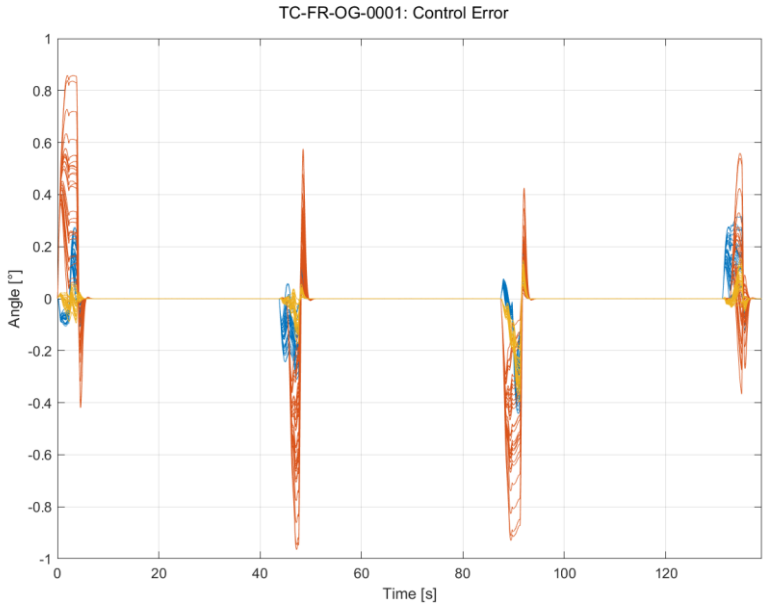

Figure 6: Control error.

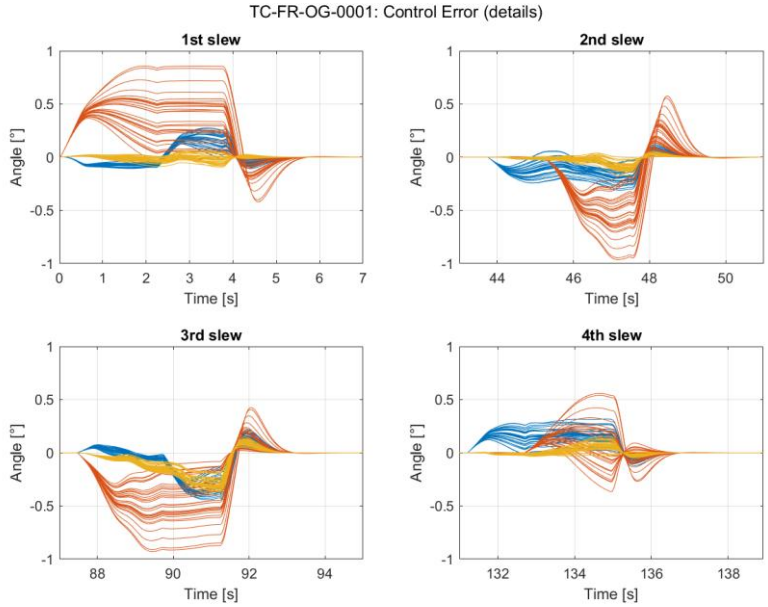

Figure 7: Control error (details).

Pointing error

The pointing errors are summarized in the APE, the RPE over 5 s and the RPE over 10 ms.

Figure 8, Figure 9, and Figure 10 show the respective APE and RPE during each of the three observation intervals. The figures indicate, in black dashed lines, the error requirement and the observation interval for which the APE and RPE requirements are fulfilled.

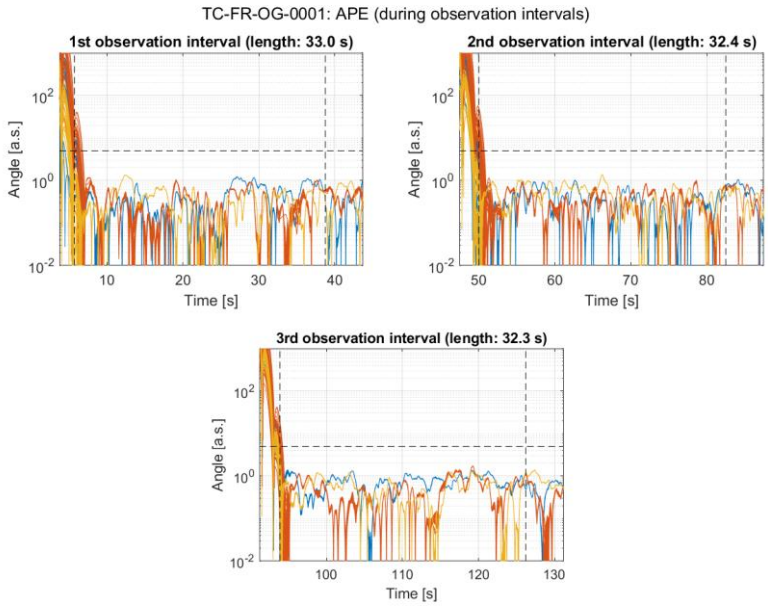

Figure 8: APE (details during observation intervals).

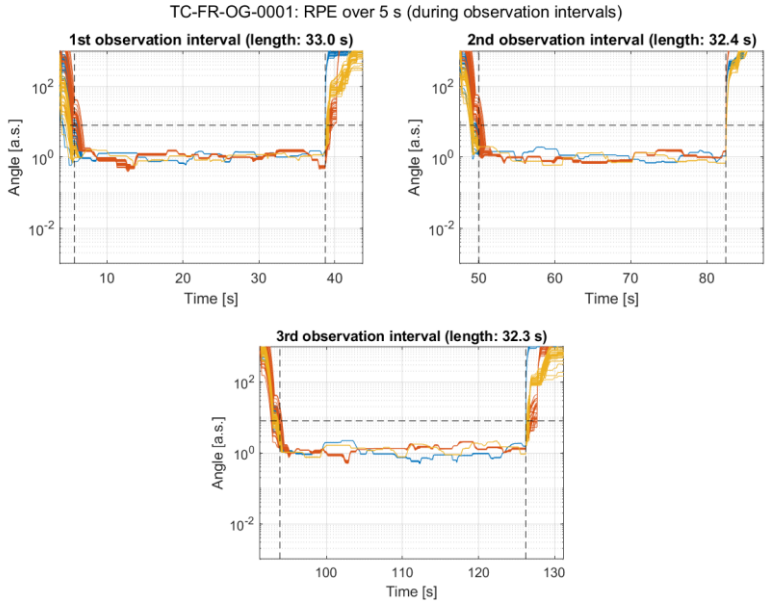

Figure 9: RPE over 5 s (details during observation intervals).

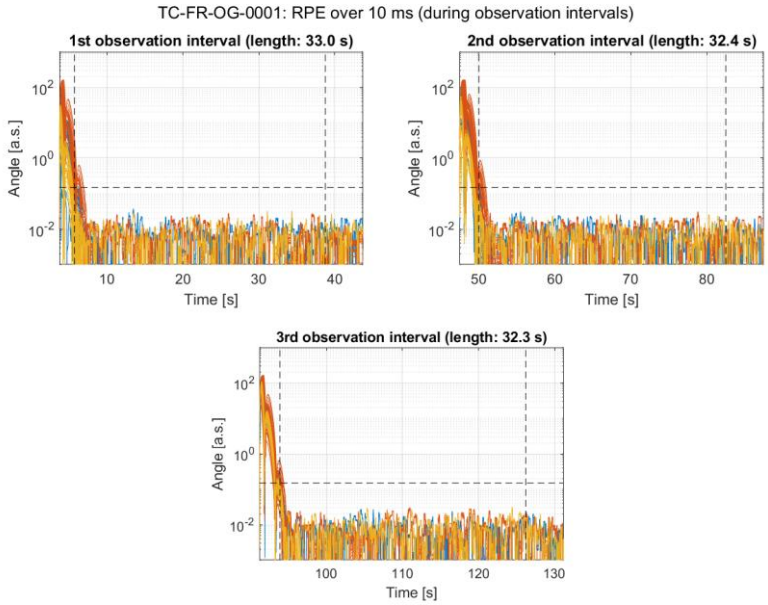

Figure 10: RPE over 10 ms (details during observation intervals).

Commanding

Figure 11 shows the simulated gimbal angles over the whole mission. Figure 12, Figure 13, Figure 14, and Figure 15 show the simulated and commanded gimbal angles for each of the four slew maneuvers. The difference between the simulated and the commanded gimbal angles is a result of both the commanding errors and the gimbal rate commands that are a result of the feedback attitude controller.

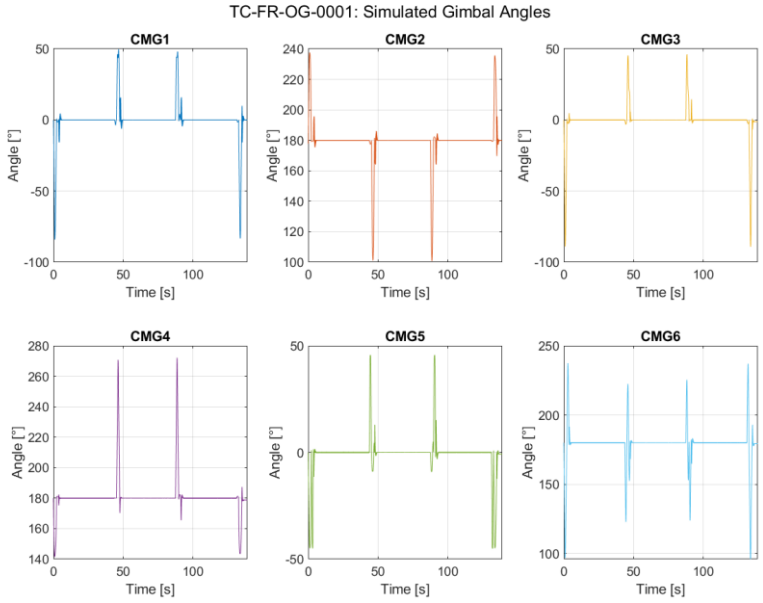

Figure 11: Simulated gimbal angles.

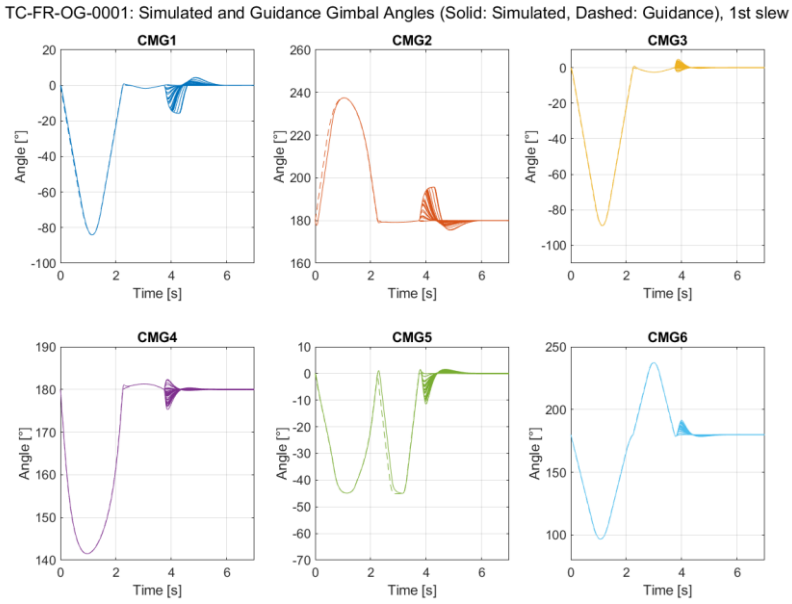

Figure 12: Simulated and guidance gimbal angles, 1st slew.

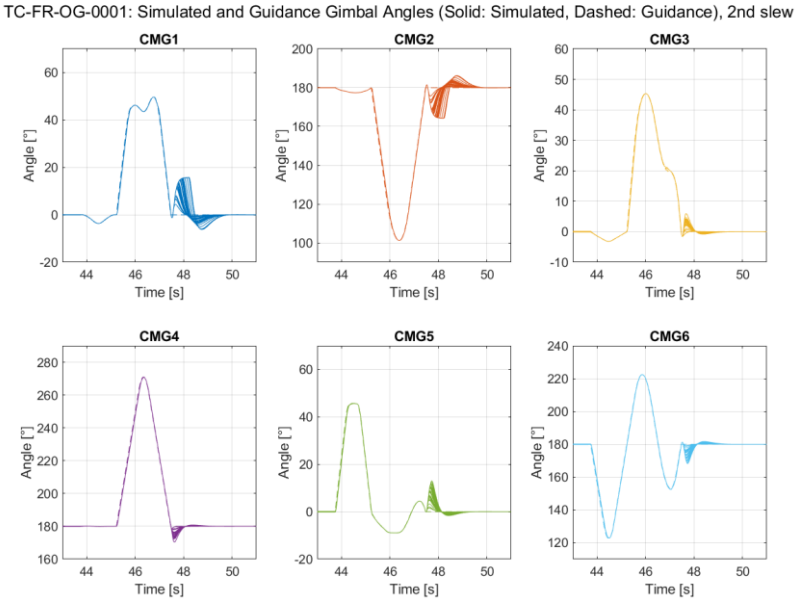

Figure 13: Simulated and guidance gimbal angles, 2nd slew.

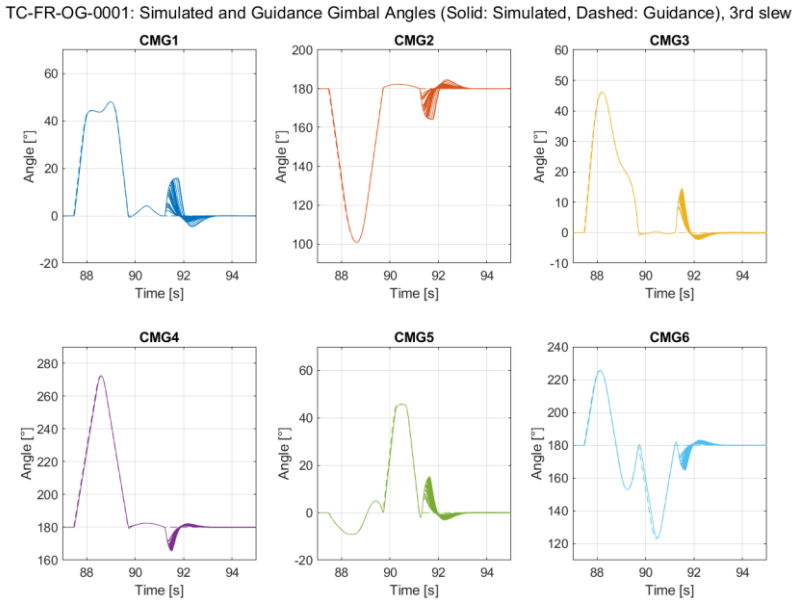

Figure 14: Simulated and guidance gimbal angles, 3rd slew.

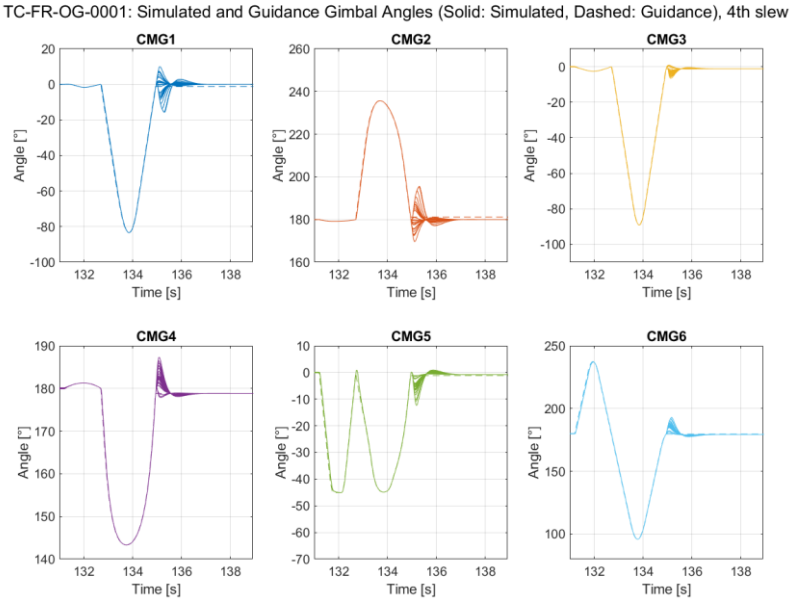

Figure 15: Simulated and guidance gimbal angles, 4th slew.

Figure 16, Figure 17, Figure 18, and Figure 19 show the simulated gimbal rates for each of the four slew maneuvers. The dashed lines indicate the saturation limit of 90°/s for the CMG units. The figures show that the saturation bound is reached for several of the CMG units.

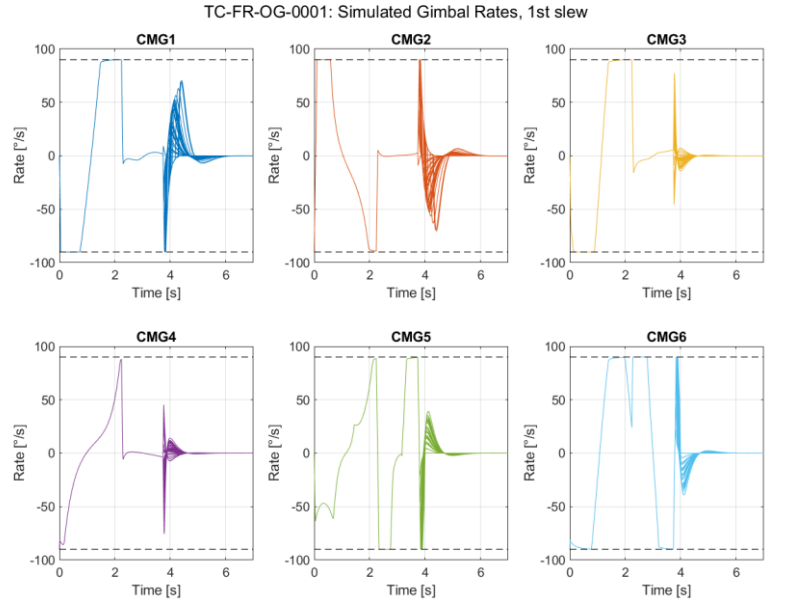

Figure 16: Simulated gimbal rates, 1st slew.

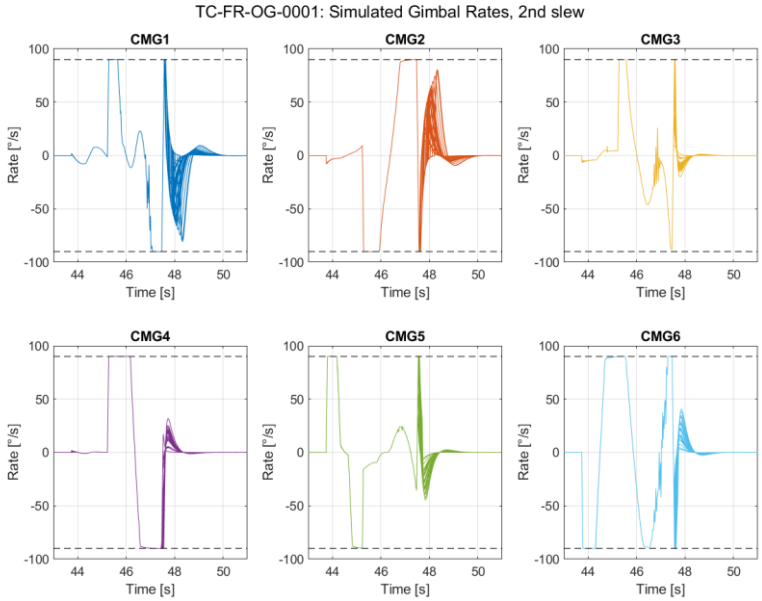

Figure 17: Simulated gimbal rates, 2nd slew.

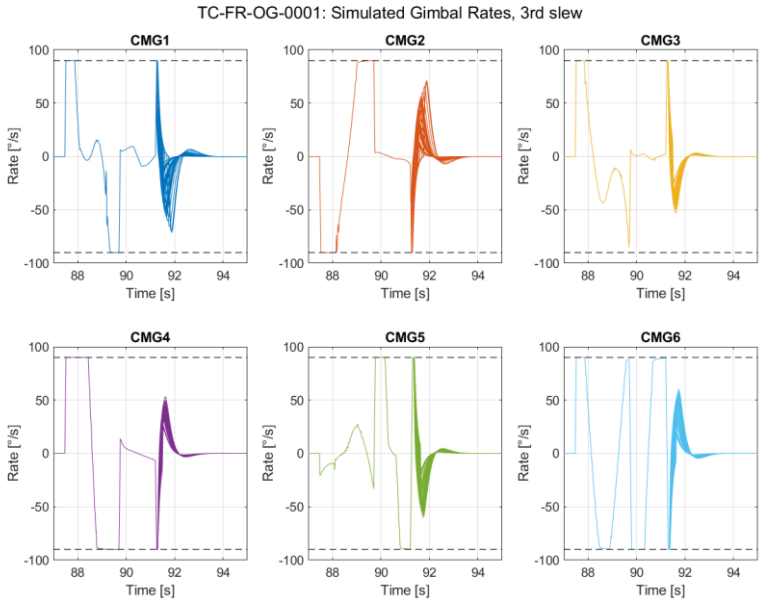

Figure 18: Simulated gimbal rates, 3rd slew.

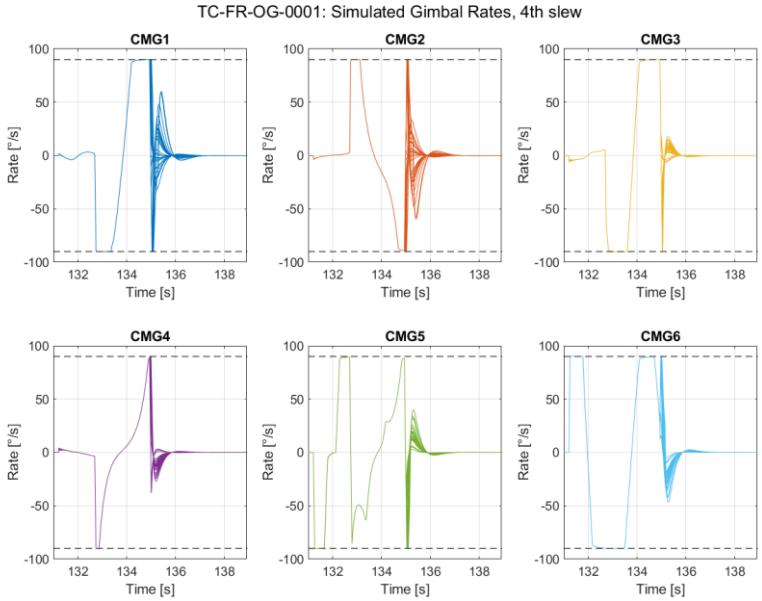

Figure 19: Simulated gimbal rates, 4th slew.

Slew Durations

The obtained slew durations are summarized in Table 2. The table demonstrates the "performance" slew durations computed from the simulation results. The duration is computed based on the attained APE and short-term RPE. The 5s RPE is not included since it has an impact on the end of the observation interval due to its low-pass characteristic. The duration of the slew of the guidance profiles is also provided in the table. The figures above show that there is a control transient of approximately 2-3 s that follows the completion of the slew guidance profile. This transient is in this way the tranquilization time needed before the actual observations can begin. The performance slew duration includes in this way also the tranquilization time. Considering this fact, the times summarized in Table 2 are well in line with the slew times of the optimized guidance profiles.

A more detailed controller implementation will include better saturation handling including integrator wind-up protection and is likely to allow further reduction of the transient duration.

Slew #	Performance slew duration including tranquilization [s]	Guidance slew duration [s]
1	5.87	3.74
2	6.82	3.73
3	5.89	3.73
4	5.77	3.73

Table 2: Summary of slew durations.

7 CONCLUSION

The study has resulted in some main conclusions, which are very briefly summarized as follows:

Overall optimization of the attitude guidance and CMG control altogether results in slightly better performance than with separate treatment of the attitude control problem and the CMG guidance

problem, both in the case of optimization-based approaches of the separated problem and in the case of an approach that is based on adaptive control.

However, solving the large nonconvex optimization problem for combined treatment of attitude and CMG guidance (SatGui0) seems to be computationally too demanding for onboard application using a CPU like the Zynq-7000. Furthermore, the optimization-based approach is sensitive to initial conditions which will result in a need of ground-based support tools for planning and generation of initial conditions. For applications that only require rest-to-rest maneuvers around a single axis the Eigenslew with predictive planning of satellite rotation angle and CMG gimbal (SatGui23) is deemed the next best alternative.

The conducted simulations were based on open loop slews using the SatGui0 strategy in combination with a closed loop a tracking controller for the observation phases. The end-to-end performance is well in line with the guidance profiles considering the additional tranquilization time associated with the transient of the attitude control upon activation of the closed loop. The transient time can most likely be further reduced with more advanced handling of command saturation in the attitude controller typically involving protection against wind-up effects.

The CMG gimbal acceleration is also identified as a limitation, and future investigations should include possible improvements from including angular acceleration limits in the guidance optimization.

8 ACKNOWLEDGEMENTS

This work was supported through funding from the European Space Agency's Technology Development Element (TDE) programme (ESA Contract No. 4000137024/21/NL/MGu "Autonomous and Optimized Agile Attitude Control with CMGs for Small Satellites Platforms").

9 REFERENCES

[1] L. Vandenberghe and S. Boyd, "Semidefinite Programming," *SIAM Review*, vol. 38, no. 1, pp. 49–95, 1996, doi: 10.1137/1038003.

[2] M. S. Lobo, L. Vandenberghe, S. Boyd, and H. Lebret, "Applications of Second-Order Cone Programming," *Linear Algebra and its Applications*, vol. 284, no. 1–3, pp. 193–228, 1998, doi: 10.1016/S0024-3795(98)10032-0.

[3] B. Acikmese and S. R. Ploen, "Convex Programming Approach to Powered Descent Guidance for Mars Landing," *Journal of Guidance, Control, and Dynamics*, vol. 30, no. 5, pp. 1353–1366, Sep. 2007, doi: 10.2514/1.27553.

[4] L. Blackmore, B. Acikmese, and D. P. Scharf, "Minimum-Landing-Error Powered-Descent Guidance for Mars Landing Using Convex Optimization," *Journal of Guidance, Control, and Dynamics*, vol. 33, no. 4, pp. 1161–1171, Jul. 2010, doi: 10.2514/1.47202.

[5] Marco Sagliano, "Pseudospectral Convex Optimization for Powered Descent and Landing," *Journal of Guidance, Control and Dynamics*, vol. 41, no. 2, 2018, doi: 10.2514/1.G002818.

[6] L. Blackmore, "Autonomous Precision Landing of Space Rockets," *The Bridge*, vol. 4, no. 46, 2019, [Online]. Available: https://www.nae.edu/164334/Autonomous-Precision-Landing-of-Space-Rockets

[7] A. Wenzel, M. Sagliano, and D. Seelbinder, "Performance Analysis of Real-Time Optimal Guidance Methods for Vertical Take-off, Vertical Landing Vehicles," in *69th International Astronautical Congress*, in Proceedings of the International Astronautical Congress, IAC. 2018.

[8] M. Dumke, G. F. Trigo, M. Sagliano, P. Saranrittichai, and S. Theil, “Design, Development, and Flight Testing of the Vertical Take-off and Landing GNC Testbed EAGLE,” *CEAS Space Journal*, vol. 12, no. 1, pp. 97–113, Aug. 2019, doi: 10.1007/s12567-019-00269-5.

[9] Z. Wang and M. J. Grant, “Hypersonic Trajectory Optimization by Sequential Semidefinite Programming,” in *AIAA Atmospheric Flight Mechanics Conference*, in AIAA SciTech Forum. American Institute of Aeronautics and Astronautics, Jan. 2017. doi: 10.2514/6.2017-0248.

[10] Z. R. Manchester and M. A. Peck, “Recursive Inertia Estimation with Semidefinite Programming,” in *AIAA Guidance, Navigation, and Control Conference*, in AIAA SciTech Forum. American Institute of Aeronautics and Astronautics, Jan. 2017. doi: 10.2514/6.2017-1902.

[11] S. Boyd, L. E. Ghaoui, E. Feron, and V. Balakrishnan, *Linear Matrix Inequalities in System and Control Theory*. Society for Industrial and Applied Mathematics, 1994. doi: 10.1137/1.9781611970777.

[12] P. Gahinet and P. Apkarian, “A Linear Matrix Inequality Approach to H-infinity Control,” *International Journal of Robust and Nonlinear Control*, vol. 4, no. 4, pp. 421–448, 1994, doi: 10.1002/rnc.4590040403.

[13] L. Vandenberghe, S. Boyd, and S.-P. Wu, “Determinant Maximization with Linear Matrix Inequality Constraints,” *SIAM J. Matrix Anal. & Appl.*, vol. 19, no. 2, pp. 499–533, Apr. 1998, doi: 10.1137/S0895479896303430.

[14] S. Boyd and L. Vandenberghe, *Convex Optimization*. The Edinburgh Building, Cambridge, CB2 8RU, UK: Cambridge University Press, 2004. [Online]. Available: http://www.stanford.edu/~boyd/cvxbook/

[15] X. Liu, Z. Shen, and P. Lu, “Entry Trajectory Optimization by Second-Order Cone Programming,” *Journal of Guidance, Control, and Dynamics*, vol. 39, no. 2, pp. 227–241, 2015, doi: 10.2514/1.G001210.

[16] Y. Mao, M. Szmuk, and B. Acikmese, “Successive Convexification of Non-Convex Optimal Control Problems and Its Convergence Properties,” in *2016 IEEE 55th Conference on Decision and Control (CDC)*, IEEE, Dec. 2016. doi: 10.1109/cdc.2016.7798816.

[17] Y. Mao, D. Dueri, M. Szmuk, and B. Açıkmeşe, “Successive Convexification of Non-Convex Optimal Control Problems with State Constraints,” *IFAC-PapersOnLine*, vol. 50, no. 1, pp. 4063–4069, Jul. 2017, doi: 10.1016/j.ifacol.2017.08.789.

[18] Y. Mao, M. Szmuk, X. Xu, and B. Acikmese, “Successive Convexification: A Superlinearly Convergent Algorithm for Non-Convex Optimal Control Problems,” 2018, doi: 10.48550/ARXIV.1804.06539.

[19] T. P. Reynolds *et al.*, “SOC-i: A CubeSat Demonstration of Optimization-BasedReal-time Constrained Attitude Control,” in *IEEE Aerospace Conference*, Big Sky MT, USA: IEEE, 2021.

[20] R. Bonalli, A. Cauligi, A. Bylard, and M. Pavone, “GuSTO: Guaranteed Sequential Trajectory Optimization via Sequential Convex Programming,” Mar. 2019.

[21] Ch. Zillober, K. Schittkowski, and K. Moritzen, “Very Large Scale Optimization by Sequential Convex Programming,” *Optimization Methods and Software*, vol. 19, no. 1, pp. 103–120, Feb. 2004, doi: 10.1080/10556780410001647195.

[22] A. Domahidi, E. Chu, and S. Boyd, “ECOS: An SOCP Solver for Embedded Systems,” in *European Control Conference*, 2013. doi: 10.23919/ECC.2013.6669541.

[23] D. Dueri, B. Acikmese, D. P. Scharf, and M. W. Harris, “Customized Real-Time Interior-Point Methods for Onboard Powered-Descent Guidance,” *Journal of Guidance, Control, and Dynamics*, pp. 1–16, Aug. 2016, doi: 10.2514/1.G001480.

[24] D. S. Elliott, “Momentum Control Systems and their Application in Robotic Systems,” PhD Thesis, Cornell University, 2019.

[25] D. S. Elliott, M. A. Peck, and I. Nesnas, “Novel Method for Control Moment Gyroscope Singularity Avoidance Using Constraints,” in *2018 AIAA Guidance, Navigation, and Control Conference*, Kissimmee, Florida: American Institute of Aeronautics and Astronautics, Jan. 2018. doi: 10.2514/6.2018-1327.

[26] D. Sawyer Elliott, M. Peck, and I. A. D. Nesnas, “Optimal Solution for Torque Capability of Control Moment Gyroscopes,” in *2019 IEEE Aerospace Conference*, Big Sky, MT, USA: IEEE, Mar. 2019, pp. 1–17. doi: 10.1109/AERO.2019.8742213.

[27] D. S. Elliott, M. A. Peck, and I. Nesnas, “Control Momentum Gyroscope Steering Law for Box-90 Array with Performance Guarantees,” in *AIAA Scitech 2020 Forum*, Orlando, FL: American Institute of Aeronautics and Astronautics, Jan. 2020. doi: 10.2514/6.2020-1101.

[28] M. A. Peck, B. J. Hamilton, and B. Underhill, “Method and System for CMG Array Singularity Avoidance,” US007246776B2

[29] R. Geshnizjani, “Zonotope Based Steering Laws for Agile Spacecraft with Control Moment Gyros,” PhD Thesis, Universität Stuttgart, 2022.

[30] R. Geshnizjani, A. Kornienko, T. Ziegler, J. Loehr, and W. Fichter, “Optimal Initial Gimbal Angles for Agile Slew Maneuvers with Control Moment Gyroscopes,” in *AIAA Scitech 2019 Forum*, San Diego, California: American Institute of Aeronautics and Astronautics, Jan. 2019. doi: 10.2514/6.2019-0936.

[31] R. Geshnizjani, A. Kornienko, T. Ziegler, J. Löhr, and W. Fichter, “Torque Optimal Steering of Control Moment Gyroscopes for Agile Spacecraft,” *Journal of Guidance, Control, and Dynamics*, vol. 44, no. 3, pp. 629–640, Mar. 2021, doi: 10.2514/1.G005118.

[32] J. Ramírez and L. Hewing, “Sequential Convex Programming for Optimal Line of Sight Steering in Agile Missions,” Jun. 13, 2022, *arXiv*: arXiv:2206.06061. Accessed: Aug. 16, 2024. [Online]. Available: http://arxiv.org/abs/2206.06061

[33] B. Wie, *Space Vehicle Dynamics and Control, Second Edition*. Reston ,VA: American Institute of Aeronautics and Astronautics, 2008. doi: 10.2514/4.860119.

[34] N. S. Bedrossian, J. Paradise, E. V. Bergmann, and D. Rowell, “Steering law design for redundant single-gimbal control moment gyroscopes,” *Journal of Guidance, Control, and Dynamics*, vol. 13, no. 6, pp. 1083–1089, Nov. 1990, doi: 10.2514/3.20582.

[35] C. Wampler, “Manipulator Inverse Kinematic Solutions Based on Vector Formulations and Damped Least-Squares Methods,” *IEEE Trans. Syst., Man, Cybern.*, vol. 16, no. 1, pp. 93–101, Jan. 1986, doi: 10.1109/TSMC.1986.289285.

[36] B. Wie, “Singularity Escape/Avoidance Steering Logic for Control Momentum Gyros,” WO2004/032392A2

[37] T. A. Johansen and T. I. Fossen, “Control allocation—A survey,” *Automatica*, vol. 49, no. 5, pp. 1087–1103, May 2013, doi: 10.1016/j.automatica.2013.01.035.

[38] ESA-ESTEC, “Attitude Guidance Using Onboard Optimization,” *Statement of Work. ESA-TECSA-SOW-01998*, 2020.

[39] V. Preda, A. Hyslop, and S. Bennani, “Optimal Science-Time Reorientation Policy for the Comet Interceptor Flyby via Sequential Convex Programming,” *CEAS Space Journal*, vol. 14, no. 1, pp. 173–186, Jun. 2021, doi: 10.1007/s12567-021-00368-2.

[40] “IOD/IOV Project 1 - Element 2.”

[41] “ELOIS Datasheet.” [Online]. Available: https://www.amos.be/wp-content/uploads/amos_elois_datasheet.pdf

[42] V. Moreau *et al.*, “EIS: A Unique Hyperspectral Pathfinder Mission Combining the Compact ELOIS Instrument and the InnoSat Smallsat Platform,” presented at the 36th annual Small Satellite Conference, Logan, UT, 2022.

[43] R. Votel and D. Sinclair, “Comparison of Control Moment Gyros and Reaction Wheels for Small Earth-Observing Satellites,” presented at the 26th annual Small Satellite Conference, Logan, UT, 2012.

[44] A. Gaude and V. Lappas, “Design and Structural Analysis of a Control Moment Gyroscope (CMG) Actuator for CubeSats,” *Aerospace*, vol. 7, no. 5, p. 55, May 2020, doi: 10.3390/aerospace7050055.

[45] A. R. Mkrtychyan, N. I. Bashkeev, D. O. Yakimovskii, D. I. Akashev, and O. B. Yakovets, “Control moment gyroscopes for spacecraft attitude control systems: Current status and prospects,” *Gyroscopy Navig.*, vol. 6, no. 3, pp. 236–240, Jul. 2015, doi: 10.1134/S2075108715030116.

[46] B. J. Hamilton, “Sizing and steering CMG arrays for agile spacecraft,” presented at the ESA GNC 2017: 10th International ESA Conference on Guidance, Navigation & Control Systems, May 2017.